International Journal of Automotive Technology, Vol. 8, No. 1, pp. 49–57 (2007)

1229-9138/2007/032-07

VEHICLE LONGITUDINAL AND LATERAL STABILITY ENHANCEMENT USING A TCS AND YAW MOTION CONTROLLER

J.-H. SONG*, H.-S. KIM and B.-S. KIM

Inje University Technology Innovation Center for Automobile Parts, School of Mechanical & Automotive Engineering, Inje University, Gyeongnam 621-749, Korea

(Received 28 June 2006; Revised 14 November 2006)

ABSTRACT–This paper proposes a traction control system (TCS) that uses a sliding mode wheel slip controller and a PID throttle valve controller. In addition, a yaw motion controller (YMC) is also developed to improve lateral stability using a PID rear wheel steering angle controller. The dynamics of a vehicle and characteristics of the controllers are validated using a proposed full-car model. A driver model is also designed to steer the vehicle during maneuvers on a split μ road and double lane change maneuver. The simulation results show that the proposed full-car model is sufficient to predict vehicle responses accurately. The developed TCS provides improved acceleration performances on uniform slippery roads and split μ roads. When the vehicle is cornering and accelerating with the brake or engine TCS, understeer occurs. An integrated TCS eliminates these problems. The YMC with the integrated TCS improved the lateral stability and controllability of the vehicle.

KEY WORDS : TCS (Traction control system), Vehicle model, YMC (Yaw motion controller), Yaw rate, Split μ road

NOMENCLATURE

a	: distance from center of gravity to the front wheel
b	: distance from center of gravity to the rear wheel
c_α	: cornering stiffness
F_n	: normal force
F_y	: lateral force
F_{roll}	: rolling resistance force
H_u	: fuel heating value
I_e	: engine and load moment of inertia
I_t	: tire moment of inertia
I_w	: wheel moment of inertia
m_f	: amount of fuel injection
m_{total}	: vehicle mass
n	: engine rotational speed (rpm)
P_B	: load power
P_L	: loss power
R_b	: distance from center of wheel to brake path
R_w	: wheel radius
T_b	: brake torque
T_{roll}	: tire rolling resistance torque
T_s	: driving axle shaft torque
x	: vehicle displacement
δ	: steering angle
ϕ	: roll angle
γ	: yaw angle
η_i	: engine thermal efficiency
η_d	: drive train efficiency
λ_{di}	: desired slip
μ	: friction coefficient
θ	: wheel angle
θ_t	: throttle valve position
τ_d	: injection time delay
ω_w	: wheel velocity
ζ_i	: gear ratio
ζ_f	: final gear ratio

*Corresponding author. e-mail: mechsong@inje.ac.kr

1. INTRODUCTION

Like the problems caused by locked wheels in braking, spinning power wheels can lead to highly reduced steerability in front-wheel-drive vehicles and a loss of stability in rear-wheel-drive vehicles (Li *et al.*, 2001). In some situations, (*e.g.*, overtaking) optimal acceleration, especially on low μ surfaces, can be an important safety factor. Beyond this, a spinning wheel under asymmetrical road conditions can prevent all forward movement.

Many researchers have developed control strategies to improve the performance of TCS (Li *et al.*, 2001; Song and Boo, 2003; Cheok *et al.*, 1996; Ryu *et al.*, 2006). Although these have obtained satisfactory results for longitudinal maneuvers, they cannot guarantee vehicle stability for lateral motion. Bang *et al.* (2001) developed a yaw controller that controls the yawing motion by

generating additional braking pressure on the outer front wheel when the vehicle is turning. Ikushima and Sawase (1995) also proposed a brake torque distribution controller to enhance lateral motion. However, these strategies concentrated on controlling the brake force and can negatively affect the driveability and steerability.

This paper proposes a new yaw motion controller (YMC) with a TCS that controls the steering angle of the rear wheels. Recent developments and research show that four-wheel steering (4WS) systems can effectively improve the handling behavior of vehicles (Siahkalroudi and Naraghi, 2002; Manning *et al.*, 2002). Such systems are easy to combine with ABS and TCS.

This paper is divided into three parts: discussions of 1) the design of a vehicle dynamic model, 2) the development of a TCS controller, and 3) the construction of a rear wheel controller. The vehicle model can be used to predict vehicle motions for steering, accelerating, and braking maneuvers. The control strategy of the TCS is to obtain greater longitudinal stability when the vehicle is accelerating. The purpose of the YMC rear-wheel steering controller is to improve the dynamic characteristics when the vehicle is turning.

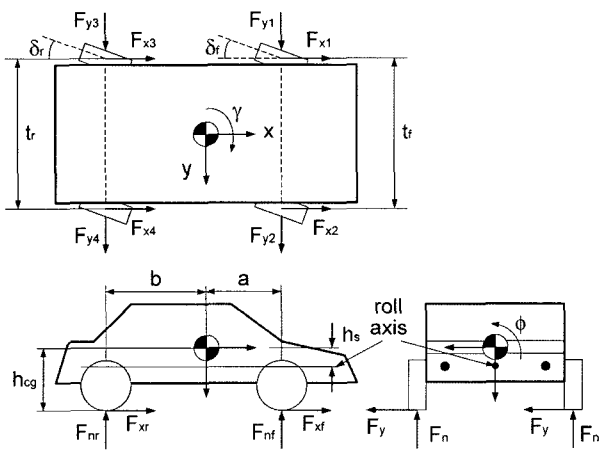

Figure 1. Vehicle model.

Table 1. Vehicle and controller design parameters.

H_u	43000 kJ/kg	I_e	0.48 kgm^2
I_w	2.1 kgm^2	R_b	0.16 m
R_w	0.3 m	a_1	1
a_2	12	a_3	0.02
A_w	0.0013 m^2	c_α	20000 N/rad
a	1.203 m	b	1.217 m
m_{total}	1280 kg	η_d	0.85
K_{pt}	1650	K_{it}	5
K_{dt}	1	K_{py}	70.2
K_{iy}	0.1	K_{dy}	0.1

2. VEHICLE DYNAMIC MODEL

A full-car model is constructed from many sub-models, such as the powertrain, suspension, tires, chassis, and so on, and the effect of each sub-system should be considered. The proposed vehicle model is used to simulate the vehicle response when steering and accelerating or steering and braking are applied simultaneously. To develop such a model, the dynamics of the vehicle must be defined by describing how the vehicle responds to given force inputs (Song and Boo, 2004). Figure 1 shows the schematics and notation of the vehicle model, and Table 1 shows the vehicle and controller design parameters.

2.1. Engine Model

The engine model used in this study is the Mean Value Engine Model (MVEM), which was introduced by Hendricks and Sorenson (1990). The MVEM describes the dynamic temporal development of the mean or average values of important observable engine variables, as well as key internal engine variables that cannot be measured directly. This model is useful for control studies and also for some engine development purposes. It is also possible to embed such engine models directly into real-time control systems.

The displacement volume of the modeled engine is 2,000 cc and the engine is equipped with an electronic multi-point fuel injection system. The equation of the crankshaft speed of the MVEM can be written as

$$n=\frac{1}{I_e \times n}(-P_L+P_B)+H_u\eta_i\dot{m}_f(t-\tau_d) \tag{1}$$

2.2. Torque Converter and Drive Shaft Model

A torque converter consists of a pump (input), turbine (output), and stator (reaction member). The pump is attached directly to the engine and therefore turns at engine speed. Torque is transferred to the turbine as a result of the oil-induced flow from the pump. The pump torque, T_p, and turbine torque, T_t, are represented as follows (Yi and Chung, 2001).

$$T_p=C_f(sr)\times\omega_e^2 \tag{2}$$

$$T_t=R_t(sr)\times T_p \tag{3}$$

where

$C_f(sr)=-1.609\times10^{-3}\,sr^2+0.2946\times10^{-3}\,sr+1.874\times10^{-3}$ (th capacity factor)

$$R_t(sr)=\begin{cases}-1.412sr+2.2 & (sr<0.85)\\ 1 & (sr\geq0.85)\end{cases}$$

(the torque ratio)

where sr is the ratio of turbine speed, ω_t, and engine speed, ω_e. The capacity factor and torque ratio of the

torque converter are represented as functions of the engine and turbine rotational speed ratio.

The driving axle shaft torque is represented as follows:

$$T_s=\frac{T_t}{\zeta_i \zeta_d} \tag{4}$$

where, ζ_i is the gear ratio of the transmission and ζ_d is the final drive gear ratio.

2.3. Vehicle Dynamics Model

A vehicle dynamics model is needed to evaluate the performance of the TCS and YMC. It consists of a chassis, tires, and brakes. The chassis model has 16 degrees of freedom (DOF), where 6 DOF are for the sprung mass, 4 DOF are for the suspension, 4 DOF are for the wheels, and 2 DOF are for the steering. Detailed information about the chassis is contained in the references (Song and Boo, 2004).

2.4. Wheel Model

The wheel dynamics model is

$$I_{wi}\dot{\omega}_{wi}=-T_b-F_{xi}r_w-T_{rolli}+T_s \tag{5}$$

where, subscript i in Equation (5) is 1, 2, 3 and 4, and represents the front left, front right, rear left, and rear right wheels, respectively.

When accelerating, the wheel inertia and half of the engine's rotational inertia are combined as

$$I_{wi}=I_{ti}+\frac{1}{2}\zeta_i^2\eta_d^2 I_e \tag{6}$$

For the non-driven wheel or when braking, the engine inertia is not included.

$$I_{wi}=I_{ti} \tag{7}$$

where, I_t is the tire moment of inertia, and η_d is the drive train efficiency.

2.5. Rolling Resistance Force

The rolling resistance force is defined as

$$F_{rolli}=f_r\times F_{ni} \tag{8}$$

where, the rolling resistance coefficient, f_r, is (Gillespie, 1992).

$$f_r=f_0+3.24f_s(K_{mph}v_{xt}/100)^{0.25}$$

where, f_o=0.0105 and f_s=0.0055 are curve-fit parameter coefficients, and K_{mph}=2.237 is a scaling constant that converts miles per hour (mph) to meters per second (m/s). v_{xt} is the speed of the wheel center in the direction that the tire is heading, and is independent for each wheel.

2.6. Wheel Slip Calculation

The TCS controllers modify the brake pressure based on the slip. Slip is defined in terms of how close each wheel is to locking. The obtainable traction or braking force depends on slip, which is defined as

$$\lambda_i=\begin{cases}\dfrac{\omega_{wi}R_w-v_{xt}}{\omega_{wi}R_w} & (acceleration)\\ \dfrac{v_{xt}-\omega_{wi}R_w}{v_{xt}} & (deceleration)\end{cases} \tag{9}$$

2.7. Friction Coefficient Calculation

The friction behavior of the wheels can be approximated using parametric characteristics. The friction, or cohesion coefficient, μ, is defined as the ratio of the frictional force acting in the wheel plane, F_{fric}, and the nomal force, F_n:

$$\mu=\frac{F_{fric}}{F_n} \tag{10}$$

The friction coefficient can be calculated using the method of Burckhardt (Kiencke and Nielsen, 2000).

$$\mu(\lambda_{Resi})=c_1\{1-\exp(-c_2\lambda_{Resi})\}-c_3\lambda_{Resi} \tag{11}$$

Where λ_{Res} is the geometrical sum of the slip and slip angle. The Burckhardt approach, Equation (11) can be extended via a pair of factors, where c_4 describes the influence of a higher drive velocity and c_5 the influence of a higher wheel load. The resulting friction coefficient is then given by:

$$\mu(\lambda_{Resi})=[c_1\{1-\exp(-c_2\lambda_{Resi})\}-c_3\lambda_{Resi}] \times\exp(-c_2\lambda_{Resi}v_{COG})\times(1-c_5F_n^2) \tag{12}$$

Where v_{COG} is the velocity of the center of gravity. Table 2 gives the parameters c_1, c_2, and c_3 for various road surfaces. Parameter c_4 ranges from 0.02 to 0.04 s/m and c_5 = 0.00151 kN^{-2}.

2.8. Driver Model

In order to close the loop in a simulation, some knowledge about human control behavior is required.

To date, descriptions of driver behavior have not been sufficiently realistic. The main problem lies in the fact that the behavior is dependant on physical and psychological factors, as well as the demands of the driving

Table 2. Parameter sets for friction coefficient characteristics.

	c_1	c_2	c_3
Asphalt, dry	1.2801	23.99	0.52
Asphalt, wet	0.857	33.822	0.347
Concrete, dry	1.1973	25.168	0.5373
Snow	0.1946	94.129	0.0646
Ice	0.05	306.39	0

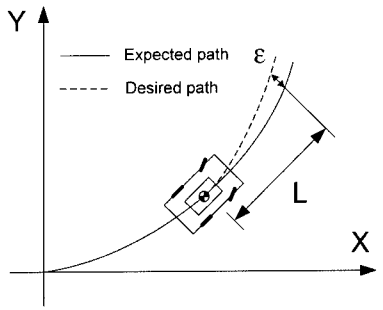

Figure 2. Strategy of the driver model

situation (Renski, 2001).

In this paper, it is assumed that the steering angle is a function of the estimated lateral offset of the vehicle center of gravity from the desired path (ε) at the look-ahead distance (L), and the yaw angle (γ) of the centre of gravity (Figure 2). This assumption can be represented mathematically as

$$\tau_s\dot{\delta}_f(t)+\delta_f(t)=\frac{a_2 v_{COG}}{(a_2+L)}\varepsilon(t)+a_3\dot{\gamma}(t) \tag{13}$$

where τ_s is the time delay of the driver's response (approximately 0.1–0.3 seconds, (Renski, 2001)), and a_1, a_2, and a_3 are constants.

3. TCS AND YAW MOTION CONTROLLER DESIGN

3.1. TCS Controller

It is possible to construct a TCS using only the braking system, like an ABS, because a brake TCS shows a very rapid reduction in the torque of the spinning wheel. However, an engine TCS is usually integrated into the system to improve traction with poor road and tire surfaces, to increase the life of the tire, brake pad, and disc, to reduce fuel consumption, and to prevent wheel spin during cornering (Sankar and Williams, 1995).

Therefore, this study proposes an integrated TCS, which is composed of a brake TCS and an engine TCS. The brake TCS uses a sliding mode wheel slip control scheme. The engine TCS controls the throttle angle with a PID control algorithm that modifies the output torque from the engine.

3.1.1. Wheel slip brake TCS

A sliding mode wheel slip controller for a TCS is very similar to that for an ABS controller. From Equation (5),

$$\dot{\omega}_i=\ddot{\theta}_i=-(K_i u_i+\tau_{xi}+\tau_{ri}-\tau_{si}) \tag{14}$$

where $K_i = A_w R_t/I_{wi}$, $\tau_{xi} = F_{xi}R_w/I_{wi}$, $\tau_{ri} = T_{rolli}/I_{wi}$, and $\tau_{si} = T_{si}/I_{wi}$.

To insure that the slip of the braking system, λ_{si}, tracks the desired slip, λ_{di}, the sliding surface is defined as

$$\begin{aligned} S&=\left(\frac{d}{dt}+\lambda\right)\int_0^t \lambda_r dr \\ &=\lambda_r+\lambda\int_0^t \lambda_r dr \end{aligned} \tag{15}$$

where λ is a strictly positive constant, r is the variable of interest and $\lambda_r = \lambda_{di} - \lambda_{si}$. The derivative of the sliding surface is

$$\begin{aligned} \dot{S}&=\dot{\lambda}_r+\lambda\lambda_r \\ &=\frac{1}{R_w\dot{\theta}_i^2}[\dot{\theta}_i\ddot{x}+(K_i u_i+\tau_{xi}+\tau_{ri}-\tau_{eng})\dot{x} \\ &\quad +R_w\dot{\theta}_i^2\lambda(\lambda_{di}-\lambda_i)] \end{aligned} \tag{16}$$

The best approximation $\hat{u}$ of a continuous control law is

$$\hat{u}_i=-\frac{1}{\dot{x}K_i}[\dot{\theta}_i\ddot{x}+(\tau_{xi}+\hat{\tau}_{ri}-\hat{\tau}_e)\dot{x}+R_w\dot{\theta}_i^2\lambda(\lambda_{di}-\lambda_i)] \tag{17}$$

Since $u_i=\hat{u}_i+\bar{u}_i$, we can define

$$\bar{u}_i=-\frac{\tau_{ri}^*+\tau_e^*+\eta}{K_i}\mathrm{sgn}(S) \tag{18}$$

where η is a strictly positive constant.

Therefore, the control input u_i can be obtained from Equations (17) and (18) as follows:

$$\begin{aligned} u_i&=\hat{u}_i+\bar{u}_i \\ &=-\frac{1}{\dot{x}K_i}[(\tau_{zi}+\hat{\tau}_{ri}-\hat{\tau}_e)\dot{x}+\dot{\theta}_i\ddot{x}+R_w\dot{\theta}_i^2\lambda(\lambda_{di}-\lambda_{si})] \\ &\quad -\frac{\tau_{ri}^*+\tau_e^*+\eta}{K_i}\mathrm{sgn}(S) \end{aligned} \tag{19}$$

A chattering problem is caused by the control discontinuity of the sgn(S) function and can be eliminated by using a thin boundary layer of thickness, Φ, next to the switching surface. Hence, sgn(S) in Equation (19) can be replaced by the function sat(S/Φ).

3.1.2. Throttle controller

The controller for the engine is used to calculate the desired value of the throttle angle, θ_i. As a result, the engine torque production tracks the desired value. The control algorithm corresponds to that of a PID controller. The desired wheel speed, ω_{wi}^*, is

$$\omega_{wi}^*=\frac{v_{xti}}{R_w(1-\lambda_{di})} \tag{20}$$

The throttle angle that minimizes the velocity error ($e_\theta = \omega_{wi}^*-\omega_{wi}$) between the desired and measured wheel speeds is calculated using a digital PID controller, for which

$$\theta_t(k)=\theta_t(k-1)+(K_{pt}+K_{it}+K_{dt})e_\theta(k) -(K_{pt}+2K_{dt})e_\theta(k-1)+K_{dt}e_\theta(k-2) \quad (21)$$

where K_{pt}, K_{it}, and K_{dt} represent the proportional, integral, and derivative gains, respectively.

3.2. PID Controller for Rear Wheel Steering

The wheel slip and throttle valve controllers were originally developed to prevent the vehicle from losing longitudinal stability while braking or accelerating. However, they have several problems, which include the fact that they induce undesirable yawing motion. These problems make it difficult for the driver to maintain safe control of the vehicle (Bang *et al.*, 2001). Therefore, this study proposes a yawing motion controller that controls the steering angle of the rear wheels.

The reference yaw rate is

$$\dot{\gamma}_{ref}=\frac{v_{COG}}{1+Kv_{COG}^2}\frac{\delta_f}{a+b} \quad (22)$$

where K is

$$K=\frac{ac_{\alpha f}\mu_f-bc_{\alpha r}\mu_r}{(c_{\alpha f}\mu_f)(c_{\alpha r}\mu_r)}\frac{m_{total}}{a+b}$$

and μ_f and μ_r are the friction coefficients of the front and rear wheels, respectively. To minimize the yaw rate error ($e_\gamma=\dot{\gamma}_{ref}-\dot{\gamma}$) between the desired and measured yaw rates, the rear wheel steering angle, δ_r, is

$$\delta_r(k)=\delta_r(k-1)+(K_{py}+K_{iy}+K_{dy})e_\gamma(k) -(K_{py}+2K_{dy})e_\gamma(k-1)+K_{dy}e_\gamma(k-2) \quad (23)$$

where K_{py}, K_{iy}, and K_{dy} are the proportional, integral, and derivative gains, respectively.

4. RESULTS AND DISCUSSION

4.1. Longitudinal Performances of the TCS on a Uniform Road

This study simulates the responses of a vehicle when it accelerates for eight seconds and maintains velocity for two seconds. It is assumed that the vehicle runs on wet asphalt or a snow-packed road, and is equipped with TCS. No steering input is entered and the vehicle is moving along a straight path.

The initial velocity is 1 m/sec and the vehicle is accelerated with the throttle valve open to 40 degrees. However, the TCS modifies the traction force by way of controlling the brake pressure and throttle angle (Figure 3). The excess traction force causes higher wheel speed, but the slip has the desired value of 0.2. The TCS generates maximum traction force on the tires. The variations in slip and brake pressure, especially if the vehicle is on wet asphalt, are from gear shifting. The lower diagrams in Figure 3 show that the brake system and throttle valve are controlled simultaneously.

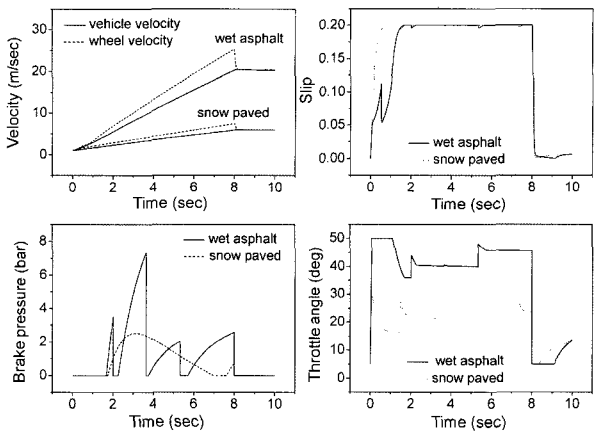

Figure 3. Performances of TCS on wet asphalt and snow paved road.

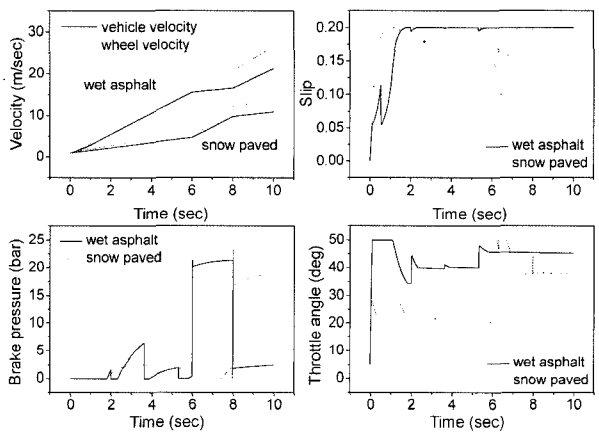

Figure 4. Performances of TCS on m change road.

4.2. Longitudinal Performances of TCS on m Change Road

The performance of the proposed TCS controller is tested with changing the road condition abruptly. Figure 4 shows the simulation result when a vehicle runs on m change road. The initial conditions are same with those of the previous study, but road conditions. The vehicle runs on wet asphalt road (snow paved road) and passes through snow paved road (wet asphalt road) from 6 to 8 seconds. The result shows that although the road condition is changed abruptly, the slip maintains the desired slip, which verifies the robustness of the TCS. When a vehicle accelerates and runs to slippery road, the brake TCS is engaged first because of faster response (Song and Boo, 2004). Thus, the brake pressure is increased. On the other hand, when the road condition is changed to the higher friction road, the brake pressure is reduced to prevent slip and the engine TCS engages.

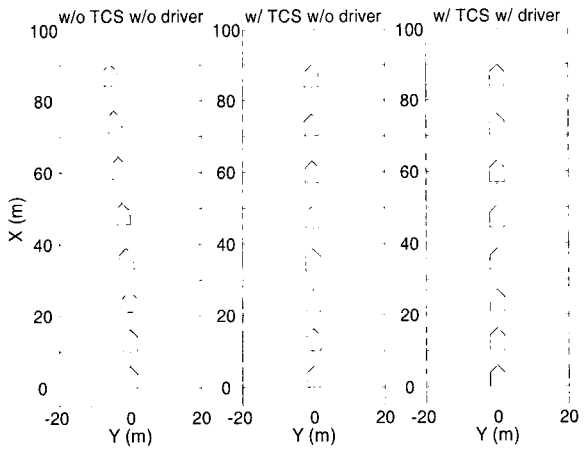

Figure 5. Trajectories of a vehicle on a split m road.

4.3. Longitudinal Performances of TCS on a Split μ Road

Figure 5 shows the trajectories of a vehicle when it accelerates suddenly on a split μ road, with the throttle valve open to 40 degrees. The initial velocity is 10 m/sec. The left wheels are assumed to be on a snow packed road and the right wheels on wet asphalt. In this condition, if the traction force is applied with no steering input applied, whether the vehicle is equipped with a TCS or not, the vehicle heads in the lower μ direction because the traction forces on both wheels differ and it is difficult to make them the same. The trajectories show that the vehicle heads toward the low μ road. However, the vehicle equipped with a TCS shows less separation than the vehicle without a TCS.

The deviation is less than 1 m over about 100 m of longitudinal movement. The trajectory of the vehicle with a TCS and a driver shows a very strong tendency to head in a straight direction.

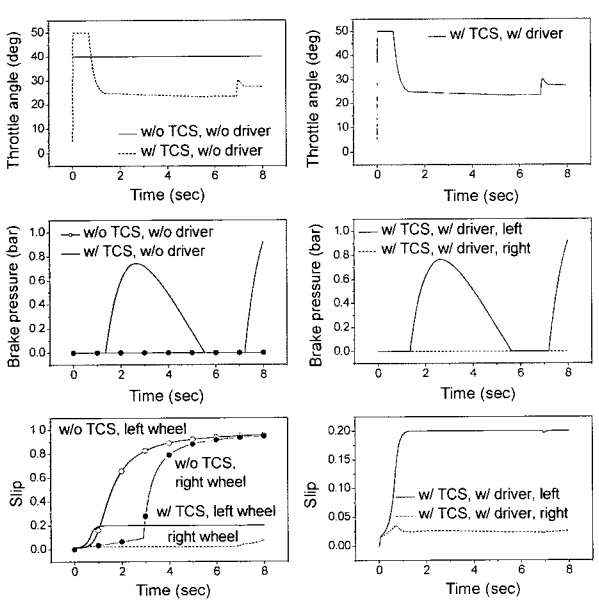

Figure 6. Performances of TCS on a split m road.

The performances of the TCS on a split μ road are shown in Figure 6. The curves on the left side of Figure 6 show the throttle angle, brake pressure, and slip when steering input is not applied. The increase in the amount of slip in the right wheel with the TCS at about 7 seconds indicates that the right wheel crosses over to the snow packed road.

The curves on the right side of Figure 6 are the responses when the driver model is applied. Since the throttle valve is controlled based on the slip of the left wheel and the brake TCS cannot modify the slip when it is less than 0.2, the slip of the right wheel cannot achieve the desired value of 0.2, as shown in the lower portion of Figure 6.

4.4. Lateral Performances of the TCS and Yaw Motion Controller

The performance of TCS, such as a brake TCS, engine TCS, or integrated TCS, are compared when the vehicle is cornering. The initial velocity is 1 m/sec and steering input is applied as represented in Figure 7. The vehicle is on wet asphalt and the initial throttle angle is 40° open.

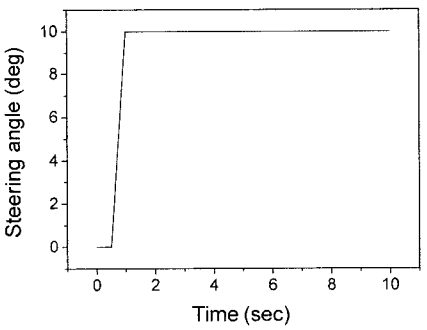

Figure 7. Steering input.

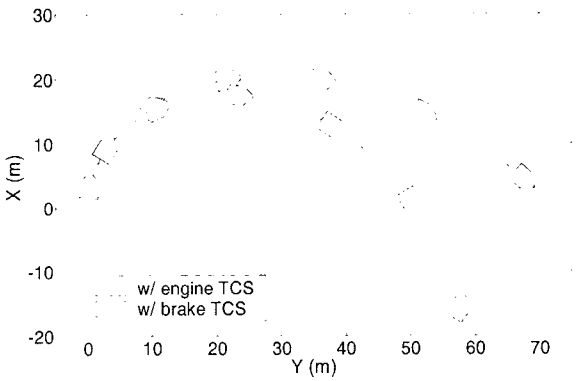

Figure 8. Trajectories of a vehicle when it equips with an engine TCS or brake TCS.

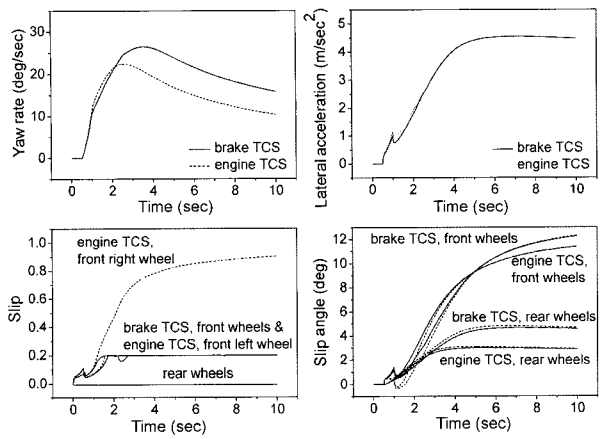

Figure 9. Performances of a vehicle when it equips with an engine TCS or brake TCS.

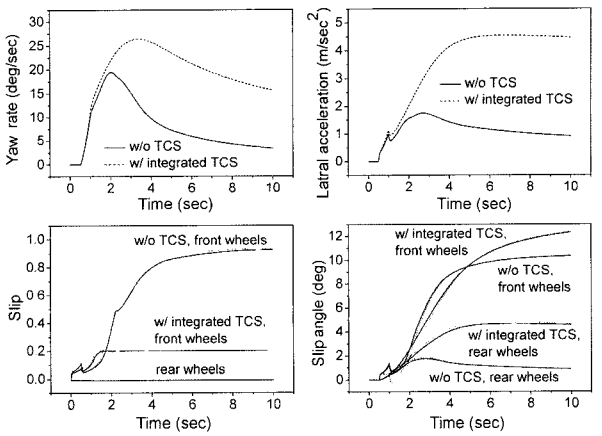

Figure 11. Performances comparison when a vehicle equips with and without an integrated TCS.

Figures 8 and 9 show the trajectories and responses when the brake TCS or engine TCS is used. The slip of the brake TCS vehicle follows the desired value. However, when the engine TCS is used, because the throttle valve is controlled based on the slip of the front left wheel, the slip of the other wheels is not as close to the desired values. This makes for a smaller yaw rate and smaller lateral acceleration, and causes a larger turning radius, as shown in Figure 8 [Song and Boo (2004)].

Figure 9 shows the performance of the brake/engine TCS vehicle. The yaw rate begins to decrease after about 3 seconds and the slip angle of the front wheel increases. The turning radius also increases, eventually resulting in understeer. The understeer takes place when the front wheels lose the available lateral force. When a vehicle accelerates, the load transfers from the front wheels to the rear wheels and lack of traction force on the front wheels causes understeer (Sankar and Williams, 1995).

Figures 10 and 11 depict the trajectories and responses of the vehicle with and without an integrated TCS. The vehicle without a TCS exhibits a large amount of slip. The yaw rate and lateral acceleration are smaller, and the turning radius is larger. Eventually, heavier understeer occurs and the vehicle becomes uncontrollable.

When an integrated TCS is adopted, the slip of the front two wheels maintains the desired value, and the lateral acceleration and yaw rates remain reasonable, indicating an improved level of steerability. The slip angle is a little larger than that of the vehicle without a TCS, but considering the much smaller turning radius, this is not a problem. However, Figure 10 shows that the integrated TCS vehicle also tends to understeer as vehicle speed increases because the turning radius increases. These results indicate that some auxiliary mechanisms are required to guarantee the controllability and stability

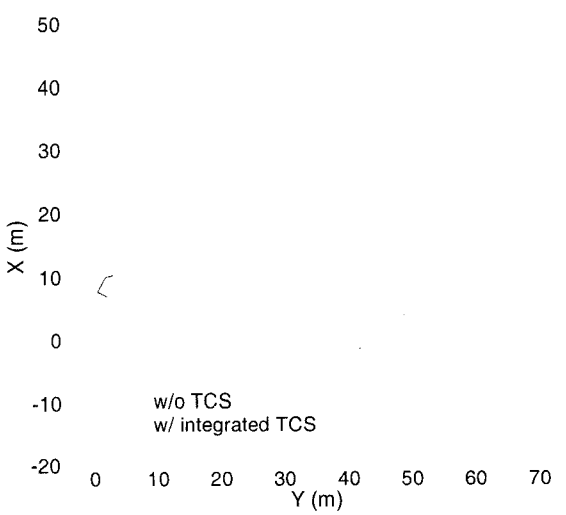

Figure 10. Trajectories comparison when a vehicle equips with and without an integrated TCS.

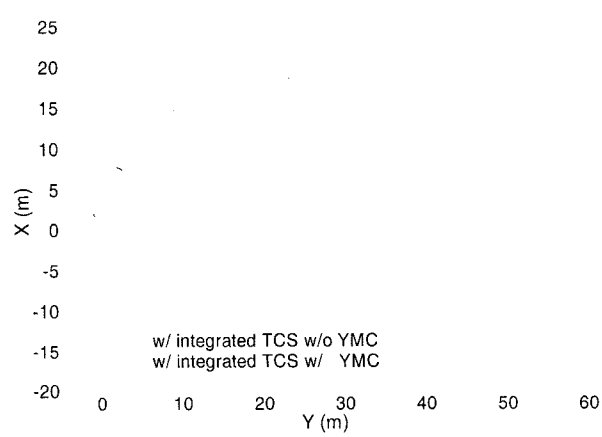

Figure 12. Trajectories comparison when TCS vehicle equips with and without YMC.

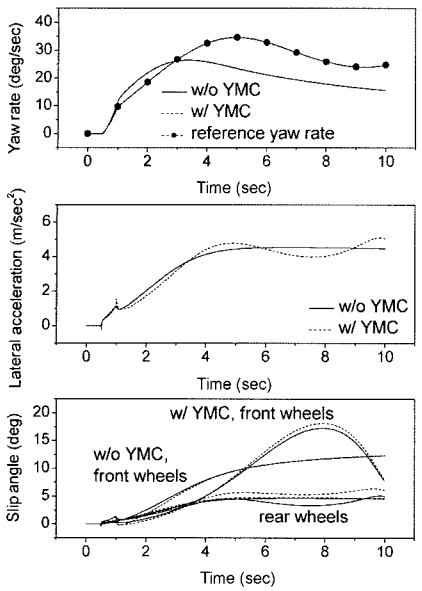

Figure 13. Performances comparison when TCS vehicle equips with and without YMC.

on wet asphalt (Sankar and Williams, 1995).

Figures 12 and 13 compare a vehicle with and without a YMC when it is equipped with an integrated TCS. The yaw rate of the YMC-equipped vehicle follows the reference yaw rate very well. It generates a higher yaw rate, which induces a smaller turning radius. The trajectories show that the yaw rate controller eliminates the understeer.

4.5. Double Lane Change of an Integrated TCS and YMC Vehicle

The performances of the driver model, integrated TCS, and YMC are validated during a double lane change maneuver. The vehicle is assumed to run on a straight, wet asphalt road with an initial velocity of 10 m/sec and the throttle valve open to 40° of acceleration in order to overtake another vehicle. Figure 14 shows the desired lateral displacement and Figure 15 depicts the trajectories of the vehicle when it is equipped with an integrated TCS alone or an integrated TCS and YMC.

As shown in Figure 15, the vehicle performs the double lane change maneuver on a wet asphalt road and follows the desired lateral displacement almost perfectly whether it is equipped with a YMC or not. These results also verify that the driver model can sufficiently control the vehicle to allow it to follow the desired path.

Figure 16 shows the characteristics of the vehicle. When the vehicle is YMC equipped, the variations in yaw rate and slip angle are reduced. The lateral accelerations are similar, but the small amount chattering is also reduced. These results show that the controllability and stability are improved when the YMC is used.

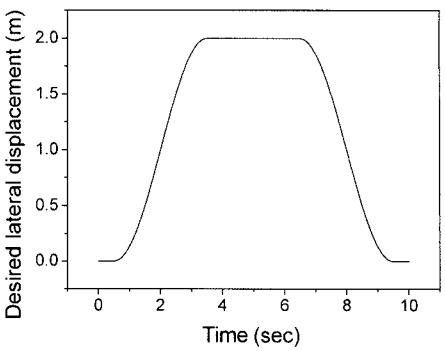

Figure 14. Desired lateral displacement to double lane change maneuver.

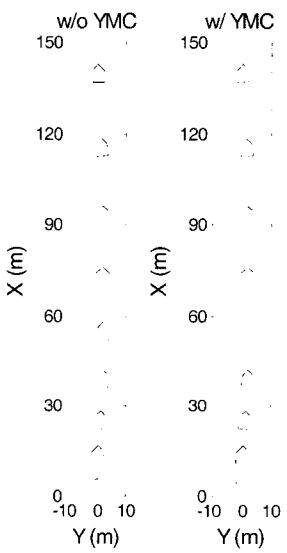

Figure 15. Trajectories of vehicle which equips with integrated TCS and YMC.

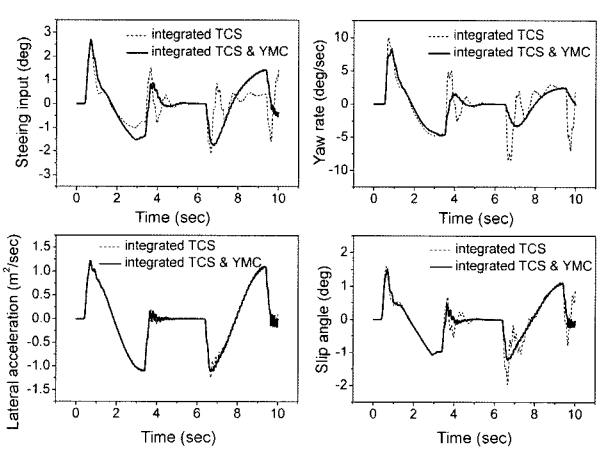

Figure 16. Performances of vehicle which equips with integrated TCS and YMC.

5. CONCLUSIONS

This simulation study investigated the performances of a TCS and YMC when the vehicle maneuvers under various conditions. These controllers are designed to enhance the stability and controllability of the vehicle. In order to perform this task, a full-car model and a driver model were also designed.

The conclusions from this study are as follows:

(1) The TCS controller works successfully when the vehicle runs on wet asphalt and snow-packed roads whether the road condition is uniform or not because the slip follows the desired value, 0.2, very well. It verifies the robustness of the TCS controller.

(2) When the vehicle is on a split μ road, the TCS reduces the deviation of the trajectories from the centerline of the road. However, it cannot prevent the deviation perfectly because it is almost impossible to control the friction force of the left and right wheels at the same time. However, when the driver model is included, the vehicle runs in the longitudinal direction without deviation.

(3) When the vehicle is in an accelerating and turning maneuver, the brake and engine TCS reduce the understeer, but they cannot perform satisfactorily. The integrated TCS shows improved results, but it cannot guarantee lateral stability. When the integrated TCS and YMC are combined, the turning radius is reduced, and the yaw rate follows the reference yaw rate very well.

(4) The driver model can allow the vehicle to follow the desired path whether the vehicle is equipped with a YMC or not. When the vehicle maneuvers through a double lane change, the YMC reduces the variation in the steering angle, yaw rate, and lateral acceleration.

REFERENCES

Bang, M. S., Lee, S. H., Han, C. S., Machiuca, D. B. and Hedrick, J. K. (2001). Performance enhancement of a sliding mode wheel slip controller by the yaw moment control. *Proc. Institute of Mechanical Engineers, Part D*, **215**, 455–468.

Cheok, K. C., Hoogterp, F. B. Fales, W. K., Kobayashi, K. and Scaccia, S. (1996). Fuzzy logic approach to traction control design. *SAE Paper No.* 960957.

Gillespie, T. D. (1992). *Fundamentals of Vehicle Dynamics*. Society of Automotive Engineers. USA.

Hendrick, E. and Sorenson, S. C. (1990). Mean value modeling of spark ignition engines. *SAE Paper No.* 900616.

Ikushima, Y. and Sawase, K. A. (1995). Study on the effects of the active yaw moment control. *SAE Paper No.* 950303.

Kiencke, U. and Nielsen, L. (2000). *Automotive Control Systems*. Society of Automotive Engineers. USA.

Li, Q., Beyer, K. W. and Zheng, Q. (2001). A model-based brake pressure estimation strategy for traction control system. *SAE Paper No.* 2001-01-0595.

Manning, W. J., Selby, M., Crolla, D. A. and Brown, M. D. (2002). IVMC: intelligent vehicle motion control. *SAE Paper No.* 2002-01-0821.

Renski, A. (2001). Identification of driver model parameters. *Int. J. Occupational Safety and Ergonomics* **7**, **1**, 79–92.

Ryu, J., Yoon, M. and Sunwoo, M. (2006). Development of a network-based traction control system, validation of its traction control algorithm and evaluation of its performance using net-HILS. *Int. J. Automotive Technology* **7, 6,** 687–695.

Sankar, M. K. and Williams, R. C. (1995). A survey of 4WD traction control systems and strategies. *SAE Paper No.* 952644.

Siahkalroudi, V. N. and Naraghi, M. (2002). Model reference tracking control of a 4WS vehicle using single and dual steering strategies. *SAE Paper No.* 2002-01-1590.

Song, J. and Boo, K. (2004). Performance evaluation of traction control systems using a vehicle dynamic model. *Proc. Institution of Mechanical Engineers, Part D*, **218**, 685–696.

Yi, K. and Chung, J. (2001). Nonlinear brake control for vehicle CW/CA systems. *IEEE/ASME Trans. Mechatronics* **6**, **1**, 17–25.